

Flight-Test Evaluation of Flutter Prediction Methods

Rick Lind*

University of Florida, Gainesville, Florida 32611-6250

Several methods have been formulated to predict the onset of flutter during flight testing. These methods have been demonstrated using data from simulations; however, a rigorous evaluation that includes data from flight testing must be performed. The ability of several methods to predict the onset of flutter by analyzing data from flight tests of the aerostructures test wing is evaluated. The evaluated methods include data-based approaches that use damping extrapolation, an envelope function, the Zimmerman–Weissenburger flutter margin, and a discrete-time autoregressive moving-average model. Also, a model-based approach that uses the μ -method flutterometer is evaluated. The data-based methods are demonstrated to be unable to predict flutter accurately using data from low-speed test points, but converge to the accurate solution as airspeed is increased. Conversely, the flutterometer is demonstrated to be immediately conservative using data from low-speed test points, but these predictions remain conservative and do not converge to the true flutter speed as the envelope is expanded. The operation of a flight test should note the properties of each method to perhaps adjust test points based on the predicted flutter margins.

Introduction

THE flight-test community routinely spends considerable time and money for envelope expansion of aircraft systems. This cost could be greatly reduced if there were a method to predict the speed associated with the onset of aeroservoelastic instabilities or the more common consideration of flutter safely and accurately.

Several methods have been developed with the goal of predicting flutter speeds and improving flight testing. These methods include approaches based on extrapolating damping trends,¹ an envelope function,² the Zimmerman–Weissenburger flutter margin,³ the flutterometer,⁴ and a discrete-time autoregressive moving average (ARMA) model.⁵ These methods have all been shown to be theoretically valid and have been demonstrated on simple test cases; however, only limited evidence exists as to their accuracy in predicting flutter during a real flight test. Flight tests have certainly been performed using the methods, but those tests rarely approached the flutter speeds. Thus, the accuracy of the predictions were not validated.

The ability to predict the onset of flutter must be carefully evaluated before an approach can reliably be used for envelope expansion. In particular, a rigorous assessment of the prediction approach must be performed with respect to aspects of flight testing that may differ from theoretical assumptions. The intention is to note the strengths and weaknesses of each method. A procedure for flight testing could then be developed that takes advantage of the strengths and avoids the weaknesses. In this way, the envelope could be expanded quickly to save costs while ensuring a high level of safety.

This paper presents an evaluation of these five methods for predicting flutter speeds. The evaluation is especially valuable because it is based on results from a flight-test program. This flight test performed an envelope expansion of the aerostructures test wing (ATW). The flight test actually used an F-15 as a host carrier for this small wing experiment. The ATW is not a complete aircraft; however, it was a complicated and realistic structure that was similar to an aircraft wing. Furthermore, the flight test was able to expand the envelope to a test point at which flutter was encountered. Thus, the

true flutter speed is known exactly and can be used to evaluate the predicted flutter speeds.

Flight data from the ATW were analyzed with respect to a constant-Mach or varying-Mach type of envelope expansion. The constant-Mach analysis considers data from test points at the same Mach number but different altitudes. Alternatively, the varying-Mach analysis considers data from test points at the same altitude but with different Mach numbers. The constant-Mach analysis is consistent with the theoretical assumptions behind the prediction algorithms, and so it is certainly a valid test of the predictive capabilities of each method. The varying-Mach analysis violates assumptions for several of the methods, but, because this type of envelope expansion may be used in practice, it is a valuable exercise to note the predictive capabilities across a limited range of Mach conditions.

The ability to predict the flutter speed for the ATW is obviously not intended to be a completely accurate assessment of each approach. The ATW has a realistic nature, but flight safety concerns required sacrifices that made this wing differ from a true aircraft wing. Also, the flutter speeds predicted from the finite element model were very sensitive to relatively small changes in mass distribution. Thus, the wing may have some ill-conditioning or scaling issues. These concerns are only small drawbacks and are overshadowed by the benefit obtained by considering such a structure in a real flight environment.

The evaluation in this paper is essentially an extension beyond a previous study.⁶ That previous study evaluated the ability of these methods to predict flutter speeds for a simulated constant-Mach flight test. This paper performs a similar type of evaluation, but uses flight data measured during an actual flight test and extends the evaluation to consider varying-Mach analysis.

Flutter Prediction Methodologies

Damping Extrapolation

The most commonly used method of predicting the onset of flutter is to extrapolate trends of modal damping.¹ This method can be considered as a data-based method because it relies entirely on analysis of flight data with no consideration of theoretical models of the specific system being tested. The data used by this method for prediction are values of modal damping ratios.

This approach is actually straightforward to understand conceptually. Simply stated, the damping of at least one mode becomes zero at the onset of flutter. The flutter prediction method consists of noting the variation in modal dampings with airspeed and extrapolating those variations to an airspeed at which damping should become zero. This resulting airspeed is considered the predicted flutter speed.

The principle behind this method is quite sound; however, there are often some difficulties in practice. One area of difficulty is the

Received 25 October 2001; revision received 18 June 2002; accepted for publication 20 June 2002. Copyright © 2002 by Rick Lind. Published by the American Institute of Aeronautics and Astronautics, Inc., with permission. Copies of this paper may be made for personal or internal use, on condition that the copier pay the \$10.00 per-copy fee to the Copyright Clearance Center, Inc., 222 Rosewood Drive, Danvers, MA 01923; include the code 0021-8699/02 \$10.00 in correspondence with the CCC.

*Assistant Professor, Department of Aerospace Engineering, 321 Aerospace Building; rick@aero.ufl.edu. Senior Member AIAA.

extraction of modal dampings. Aeroelastic flight data often have low signal-to-noise ratios, and so sophisticated techniques like parameter estimation or modal filtering may be required.⁷ Another area of difficulty is the extrapolation method. Damping can be a highly nonlinear function of airspeed so that the extrapolation must be carefully performed to ensure it accurately accounts for any high-order nonlinearity.

Envelope Function

Flutter speeds can be predicted using a method based on an envelope function,² namely, the envelope function. This method, like the damping extrapolation approach, is a data-based approach that predicts the onset of flutter based entirely on analysis of flight data. The data used by this method are simply the time-domain measurements from sensors in response to an impulse excitation.

The fundamental nature of this method is somewhat similar to the method based on damping extrapolation; however, this method does not directly use estimates of modal damping. Instead, this method notes that the envelope bounding an impulse response gets bigger as damping decreases. Thus, the size and shape of the response envelope can be used to indicate a loss of damping and, consequently, the onset of flutter.

An envelope function that bounds an impulse response can be computed in several ways. The current formulation considers an approach based on the Hilbert transform. A signal $y(t)$ is related to its Hilbert transform $y_H(t)$ as being similar in magnitude but differing in phase by 90 deg. An envelope function that bounds the impulse response is easy to compute by using the phase difference between $y(t)$ and $y_H(t)$:

$$\text{env}(t) = \sqrt{y(t)^2 + y_H(t)^2}$$

This envelope will clearly increase in size as the data indicate impulse responses of a system with decreasing modal damping. Unfortunately, the amplitude of this envelope can be also affected by the size and shape of the impulse given to the system. Thus, the time centroid is needed as a further indication of the stability of a system. This centroid \bar{t} is computed with respect to a maximum length of time window t_{\max} within which the data lie:

$$\bar{t} = \frac{\int_0^{t_{\max}} \text{env}(t) t dt}{\int_0^{t_{\max}} \text{env}(t) dt}$$

A shape parameter is used for the actual prediction of flutter. This parameter S is simply the inverse of the time centroid such that $S = 1/\bar{t}$. This shape parameter is then assumed to be a polynomial function of airspeed:

$$S = S_0 + S_1 V + S_2 V^2$$

The prediction of the flutter speed is accomplished by noting that $S = 2/t_{\max}$ when the system has critical damping at the onset of flutter. The flutter speed is, thus, predicted by noting the value of the polynomial at which this condition is satisfied.

Zimmerman–Weissenburger Margin³

Another method to predict the onset of flutter has been developed that uses the concept of a flutter margin.³ This method is also a data-based method in the sense that it only uses information obtained directly from the flight data. In this case, the flutter margin makes use of information about the poles of the transfer function obtained from the data.

The flutter margin, as originally formulated by this approach, is an indicator of distance to flutter in terms of dynamic pressure. The development of this method is based on the equations of motion for a classical aeroelastic system with bending and torsion modes. The method was formulated for a two-mode flutter mechanism but has since been extended to consider one-mode (Ref. 8) or three-mode (Ref. 9) instability.

The essence of the method is to consider the characteristic polynomial that describes the continuous-time aeroelastic system. The stability of this system can be evaluated by applying the Routh stability criterion. Assume that the system is indeed a two-mode system

with two pairs of distinct poles given by $\lambda_{1,2}$ and $\lambda_{3,4}$. Define parameters to represent the real and imaginary parts of these poles such that $\lambda_{1,2} = \beta_1 + j w_1$ and $\lambda_{3,4} = \beta_2 + j w_2$.

The flutter margin F_M is formulated by applying the Routh stability criterion to the two-mode system. This criterion results in a parameter that must be positive if the corresponding system is stable. The parameter is, thus, written in terms of the system poles:

$$F = \left[\frac{(\omega_2^2 - \omega_1^2)}{2} + \frac{\beta_2^2 - \beta_1^2}{2} \right]^2 + 4\beta_1\beta_2 \left[\frac{(\omega_2^2 + \omega_1^2)}{2} + 2 \left(\frac{\beta_2 + \beta_1}{2} \right)^2 \right] - \left[\frac{\beta_2 - \beta_1}{\beta_2 + \beta_1} \frac{w_2^2 - w_1^2}{2} + 2 \left(\frac{\beta_2 + \beta_1}{2} \right)^2 \right]^2$$

The flutter margin is obviously zero if either $\beta_1 = 0$ or $\beta_2 = 0$. This parameter is, thus, indicative of the stability of a system; however, that does not necessarily make it valuable for predicting the onset of flutter. The nature of a flutter margin arises by noting, subject to some assumptions, that the parameter F varies with dynamic pressure. Some studies have noted that this variation may be considered linear¹⁰; however, this paper will use the theoretical formulation, which assumes quadratic variation.

$$F = f_0 + f_1 \bar{q} + f_2 \bar{q}^2$$

The dynamic pressure associated with flutter is predicted by computing F from data taken at test points with different values of dynamic pressure. The roots of this equation for F give the dynamic pressure at which the onset of flutter is predicted to occur.

Flutterometer

The flutterometer is another tool to predict flutter speeds that is under study.⁴ This tool differs dramatically from the other approaches considered in this paper. The main difference arises because this tool is a model-based approach. Basically, the flutterometer uses both flight data and theoretical models to predict the onset of flutter. The flight data under consideration are frequency-domain transfer functions from sensors to an excitation. The model to be analyzed is the corresponding theoretical transfer function.

The formulation for this approach is based on μ -method analysis.¹¹ This type of analysis computes a stability measure that is robust with respect to an uncertainty description. The flutter speed is, thus, computed as the largest increase in airspeed for which the theoretical model remains robustly stable with respect to the uncertainty.

The flutterometer operates by computing a robust flutter speed at every test point. The initial step is to compute an uncertainty description for the model at that flight condition. This step is performed by noting differences between the theoretical and measured transfer functions. Uncertainty is introduced into the model as variations such that the resulting range of theoretical transfer functions bounds the measured transfer function. The next step is to compute the robust flutter speed. This step is performed by a straightforward application of μ -method analysis on the theoretical model that contains the uncertainty variations. In this way, the flutterometer predicts a realistic flutter speed that is more beneficial than theoretical predictions because the robust speed directly accounts for flight data.

A mathematical description of the flutterometer is beyond the scope of this paper. Instead, information may be obtained from the literature.⁴

Discrete-Time ARMA Modeling

A flutter prediction method has been developed that considers stability of discrete-time aeroelastic systems.⁵ This method is a data-based approach; however, the type of data used by this method

is different from the data used by the previous methods. The discrete-time approach relies on time-domain measurements from the system in response to random excitation. This type of data is usually provided by sensor measurements that record the response to atmospheric turbulence.¹²

The analysis of turbulence data presents simultaneously an advantage and disadvantage in comparison to other methods. It is convenient to allow flutter testing that does not require consistent and broadband excitation; however, it is often difficult for turbulence to generate response levels in which all modes are sufficiently observed.

This method requires data measured in response to turbulence because of assumptions about the aeroelastic system. Specifically, the system is assumed to be represented accurately by an ARMA model. This type of model uses autoregressive measurements and a moving average of white noise to describe the dynamics. The coefficients associated with the autoregressive measurements are associated with the stability characteristics. Define the characteristic polynomial $G(z)$ as a function of the discrete-time variable z . This polynomial can be expressed using standard coefficients α_i or poles z_i :

$$\begin{aligned} G(z) &= \alpha_4 z^4 + \alpha_3 z^3 + \alpha_2 z^2 + \alpha_1 z + \alpha_0 \\ &= \alpha_4 (z - z_1)(z - z_1^*)(z - z_2)(z - z_2^*) \end{aligned}$$

This form for the characteristic polynomial assumes that the dynamics are described by two modes. There are four poles in the dynamics, but they are restricted to be complex conjugate pairs.

The stability of the system is readily computed by applying the Jury determinant method. This method guarantees stability of a discrete-time system if certain conditions are satisfied. The conditions can be written in terms of the poles. There are six conditions to be satisfied for this fourth-order system; however, the condition defined as $F^-(3)$ is of particular interest:

$$F^-(3) = \alpha_4^3 (|1 - z_1 z_2|^2) (|1 - z_1 z_2^*|^2) (1 - |z_1|^2) (1 - |z_2|^2)$$

Stability of a discrete-time system is ensured if all poles have magnitudes less than unity. This result implies a stable system will always have $F^-(3) > 0$. Furthermore, the value of $F^-(3)$ goes to zero as the system approaches instability. Thus, $F^-(3)$ has been used as a stability predictor whose trends toward zero indicate the onset of flutter.¹³ Unfortunately, $F^-(3)$ was noted to have some potentially adverse behavior with dynamic pressure; therefore, the behavior of a similar parameter, $F^-(1)$, was considered:

$$F^-(1) = \alpha_4 (1 - |z_1|^2 |z_2|^2)$$

Note that the behavior of $F^-(3)$ is somewhat improved by associating it with $F^-(1)$. This forms the basis for F_z as the discrete-time ARMA flutter margin:

$$F_z = F^-(3)/F^-(1)^2$$

The flutter margin is used to predict the onset of flutter by expressing F_z as a function of flight condition. Specifically, a standard approach is to express F_z as a quadratic function of dynamic pressure:

$$F_z = f_0 + f_1 \bar{q} + f_2 \bar{q}^2$$

The dynamic pressure associated with flutter is predicted by computing F_z at several different flight conditions, computing coefficients for $F_z = f_0 + f_1 \bar{q} + f_2 \bar{q}^2$ that note the dependency on dynamic pressure, and finding the dynamic pressure at which $F(z)$ becomes zero.

The flutter speed produced by this method has some similarities to the earlier predictions. Most notably, the flutter speed predicted by this method is mathematically similar to the speed predicted by the Zimmerman–Weissenburger³ approach if certain assumptions are enforced.

Flight-Test Evaluation

Aerostructures Test Wing

The ATW was developed at NASA Dryden Flight Research Center. The ATW was essentially a wing and boom assembly as shown in Fig. 1. This assembly was flown by using an F-15 aircraft and

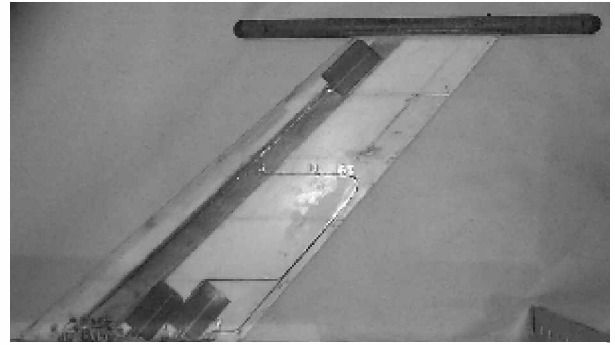


Fig. 1 Aerostructures test wing.

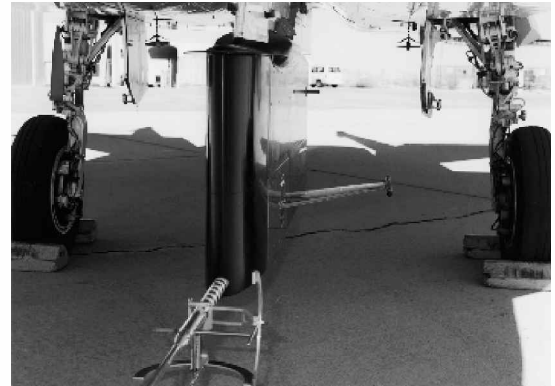


Fig. 2 Mounting of the ATW.

associated flight-test fixture. The ATW mounted horizontally to the fixture and the resulting system attached to the F-15 fuselage as shown in Fig. 2. Previous testing indicated that the airflow is relatively smooth around the system, and so the F-15 fuselage and wings are assumed to have minimal interference with the ATW.

The wing was formulated based on a NACA-65A004 airfoil shape. The wing had a span of 1.5 ft with root chord length of 1.1 ft and tip chord length of 0.725 ft. The boom was a 0.0833-ft-diam hollow tube of length 1.8 ft. The total weight of the ATW was 2.66 lb.

The ATW was meant to be a realistic testbed that represents the complexity of an aircraft component like a wing or tail; however, the construction was limited by safety concerns. These potentially conflicting issues were addressed by designing the ATW with a rib and spar construction that uses lightweight materials with no metal. Specifically, the skin and spar were constructed from fiberglass cloth, the boom was constructed from carbon fiber composite, the wing core was constructed from rigid foam, and components were attached by epoxy. Also, powdered tungsten was included in the endcaps of the boom for mass balancing. The system was designed to flutter at a subsonic condition within the flight envelope of the host F-15.

A measurement and excitation system was incorporated into the wing. The measurement system consisted of 18 strain gauges placed throughout the airfoil structure and three accelerometers placed at fore, aft, and mid locations in the boom. The excitation system was six patches of piezoelectric material, three patches mounted on the upper surface that are out of phase with three patches on the lower surface, that acted as a single distributed actuator. Sinusoidal sweeps from 5 to 35 Hz were commanded to these patches.

Ground vibration tests were conducted to determine the structural dynamics of the wing. The main modes of the system and their natural frequencies are presented in Table 1. Tests were conducted for the wing on a test stand and also attached to the flight-test fixture to ensure that these modal properties were not affected for the flight testing.

Envelope Expansion

The flight-test program followed standard procedures for envelope expansion. The system was stabilized at a test point, response

Table 1 Measured modes of the ATW during ground vibration testing

Mode	Frequency, Hz
First bending	14.05
First torsion	22.38
Second bending	78.54

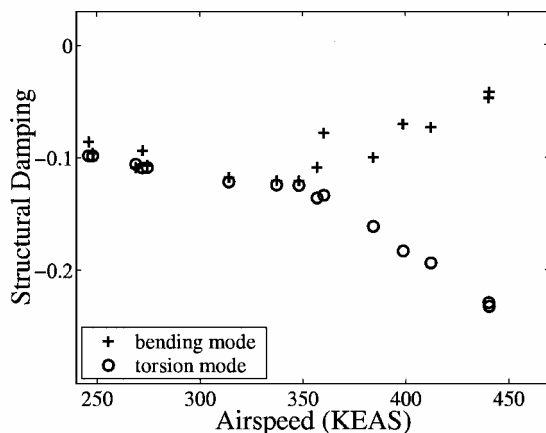


Fig. 3 Measured modal dampings.

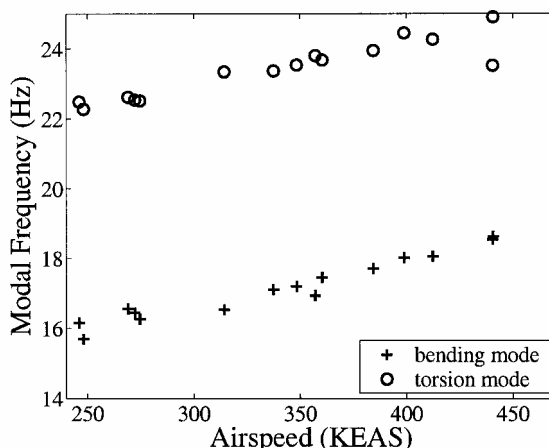


Fig. 4 Measured modal frequencies.

to turbulence excitation was recorded for 30 s, response to a sine sweep excitation through the piezoelectric patches was recorded for 60 s, then the system was accelerated to the next test point.

The ATW, in its final configuration, was flown on four flight tests. These flights included 21 test points with Mach numbers between 0.50 and 0.83 and altitudes between 10,000 and 20,000 ft. The ATW experienced a destructive flutter incident on the final flight at conditions of Mach 0.83 and 10,000 ft, which corresponds to a speed of approximately 460 kn of equivalent airspeed (KEAS).

Modal parameters were computed at each test point. The response to sinusoidal excitation was used for these computations. Transfer functions were computed from the commanded excitation to the accelerometer responses. A standard frequency-domain method of system identification was used to formulate a system model whose dynamics were similar to the measured transfer functions. The modal parameters of that model were then extracted and used as representative of the ATW parameters.

The modal dampings that were extracted at each test point are given in Fig. 3. The flutter instability affecting the bending mode is clearly evident in the data trends. Furthermore, the damping data indicates that the ATW experiences a classical type of flutter, such that one mode is becoming less stable, whereas the other mode is becoming more stable.

The modal frequencies for the ATW are given in Fig. 4. These data seem to contradict the indication that the ATW is experiencing

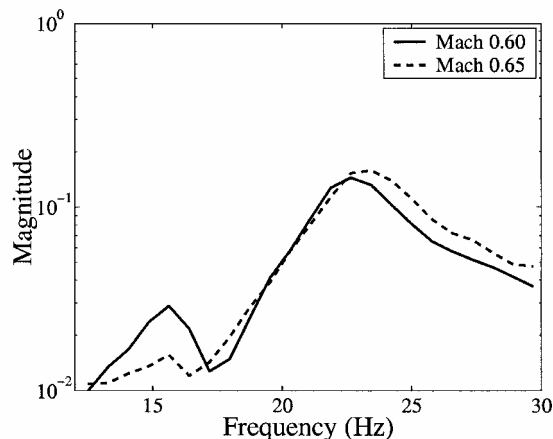


Fig. 5 Transfer functions at 20,000 ft.

a classical bending-torsion flutter. Notably, the natural frequencies do not appear to be coalescing, as expected for classical flutter, until a possible coalescence at the airspeed very close to the onset of flutter.

Data Quality

Each of the methods discussed in this paper analyzes flight data to predict the onset of flutter. The quality of the flight data are, thus, of obvious importance in evaluating the predictive nature of the approaches. Data quality is a difficult measure to describe; however, the quality of the ATW data, for purposes of flutter prediction, could be judged by the ability to observe modes.

Figure 5 presents an example of data quality as determined by modal observability. The transfer functions from the accelerometers to the excitation command are noticeably different between a test point at Mach 0.60 and 20,000 ft and a test point at Mach 0.65 and 20,000 ft. In particular, the response of the bending mode near 16 Hz is significantly less at the higher speed.

The low response levels in the data can have significant effects on flutter prediction. Essentially, several approaches for flutter prediction rely on accurate values of the modal characteristics of the system. The low response levels shown in Fig. 5 make it difficult to identify any modal characteristics for the bending mode accurately. Thus, the approaches may predict flutter speeds based on inaccurate or incomplete information.

The comparison in Fig. 5 describes only two test points; however, similar variations were noted at many test points. The bending mode was not excited or observed consistently at several test points. The problem was especially noted between Mach 0.50 and 0.70 flight conditions. At these low Mach numbers, there were at most two test points, out of the three that were flown, with good quality data.

This issue of data quality is evident in the damping plots of Fig. 3. That plot only contains 15 estimates of damping, even though the flight test consisted of 21 test points. The 15 estimates correspond to test points at which the bending mode could be sufficiently excited and observed. These test points include two points at Mach 0.50, two at Mach 0.55, one at Mach 0.60, one at Mach 0.65, three at Mach 0.70, two at Mach 0.75, three at Mach 0.80, and one at the final Mach 0.82 test point.

Prediction Algorithms

Predictions of the onset of flutter were performed using the five methods discussed in this paper. Several types of data were available for analysis. The first type of data was simply the time-domain responses of the accelerometers. The frequency-domain responses, computed by standard Fourier transforms, were also available. Additionally, a four-state system model was computed by standard system identification approaches applied to the frequency-domain data between 12 and 30 Hz (Ref. 14). Finally, the theoretical state-space model of the ATW was also available.

The method to predict flutter speed by damping extrapolation was the most straightforward to implement. The data analyzed was the

modal dampings associated with the system model identified from the frequency-domain accelerometer responses. In this case, those dampings were assumed to be a second-order function of airspeed. The flutter speed was predicted as the largest root of the second-order polynomial associated with the damping functions.

The method using the envelope function was somewhat more complex to implement than the damping method, but did not present any serious difficulties. The main issue for implementation of this method was to get a time-domain Hilbert transform of impulse-response data even though the ATW only measured data in response to sinusoidal excitation. The desired data were generated in several steps by computing the Fourier transform of the time-domain sinusoidal data, rearranging the components to compute the frequency-domain Hilbert transform of those data, and taking the inverse Fourier transform to get the time-domain Hilbert transform of an impulse response. A simple numerical integration was then used to compute the envelope function and the shape parameter as second-order functions of airspeed. The value at which this polynomial matched the flutter condition was used as the predicted flutter speed.

The flutter margin associated with the Zimmerman-Weissenburger³ approach was computed with no difficulty. This method used the real and imaginary parts of the poles of the identified system model. The flutter margin was computed from these values and modeled as a second-order function of dynamic pressure. The largest root of that polynomial was converted, using match-point flight conditions, to a value of airspeed that was used as the predicted flutter speed.

The flutterometer was implemented as the only model-based approach.¹⁵ This tool analyzed transfer functions computed from both the frequency-domain responses and the theoretical state-space models. The uncertainty levels used by the flutterometer were initially zero, but were updated at every test point to reflect errors noted by the data. The uncertainty description computed in this way related the potential errors in the model associated with the Mach number of the flight condition. A prediction of the worst-case flutter speed was computed by a robust aeroelastic stability analysis using the μ -method approach for the model with respect to that flight-derived uncertainty description.

The implementation of the method to predict flutter using a discrete-time ARMA approach was the most difficult. This method used the time-domain measurements that were obtained in response to turbulence excitation. The data were extremely noisy, and so they were processed through a low-pass filter with cutoff frequency at 160 Hz. An ARMA model was then identified to match the data using a Gauss-Newton algorithm (see Ref. 16). The development of the method assumed a two-mode system with four poles; however, the data analysis had to consider a system with six poles. In some cases, the ARMA model was identified as having two sets of complex conjugate poles and two purely real poles. The real poles were ignored and the method proceeded using the sets of complex conjugate poles. In other cases, the ARMA model was identified as having three sets of complex conjugate poles. For these cases, the two sets of poles that were closest in frequency to the measured aeroelastic modal frequencies were used for flutter prediction. In all cases, the flutter parameter was computed using the desired sets of complex conjugate poles from the ARMA model. This parameter was modeled as a second-order function of airspeed whose roots indicated the predicted onset speed of flutter.

Constant-Mach Predictions

Implementation

A common method for envelope expansion is to operate the aircraft at a series of test points along lines of constant Mach. Such testing essentially involves changing the altitude to a desired condition and then changing the airspeed to attain the desired Mach condition. The data from the ATW were processed to predict flutter speeds for this type of constant-Mach envelope expansion.

The data used for flutter prediction were restricted to consider individual Mach numbers. Each approach considered the flight data

from the test points at three different altitudes for a particular Mach number. In this way, the flutter speed for Mach 0.70 was based purely on analysis of data from Mach 0.70 flight conditions.

The approaches to predict flutter were straightforward to implement. The data-based approaches simply used the roots of various functions of airspeed measured in feet per second to determine the flutter speed. The model-based approach simply computed a robust stability analysis of the model at that Mach number with respect to an uncertainty description determined by the data at that Mach number.

The constant-Mach envelope expansion should be a valid test of the predictive capabilities of each approach. Each method was developed to consider constant-Mach conditions, and so this type of envelope expansion does not violate any assumptions associated with the theoretical basis of the predictions.

Predictions of Flutter Speeds

The flutter speeds predicted for constant-Mach envelope expansion are given in Table 2. Each row represents the predicted speeds for a particular Mach number, whereas each column gives the speed predicted by a certain method. Also, the values of V_{true} are given to represent the true flutter speeds. The flight test encountered flutter only near the Mach 0.8 condition, and so the remaining speeds are based on model characteristics and assumptions as to the behavior of the ATW.

An important feature of Table 2 is that predicted flutter speeds are not given at certain Mach numbers for some of the methods. This feature does not suggest that the method was unable to predict a flutter speed; rather, it signifies that the method predicted the speed as an imaginary or negative number. The speed in these situations is predicted by extrapolating a function whose coefficients are determined by curve fits of data. The failure to predict a valid speed is indicative of data values with properties that differed greatly from the theoretical expectations, and so the curve fit was unable to produce a reasonable function.

Another feature of Table 2 is the differences in speeds predicted by different methods. In particular, the predictions vary considerably for flight at low Mach numbers but converge to similar answers as Mach number increases. For instance, the predictions at Mach 0.55 vary from 591 to 732 ft/s, whereas the predictions at Mach 0.80 vary only from 852 to 886 ft/s.

These two features are somewhat related in that they are caused by same issue. Namely, the flight data generated at low Mach numbers were of lower quality than the data generated at high Mach numbers. The concept of modal observability is actually quite appropriate as a measure of data quality for this application. The result of the poor data quality was such that there were, at most, two high-quality data values at low Mach conditions available for a curve fit that required three values. Consequently, the resulting predictions show a fair amount of error.

The predicted flutter speeds from Table 2 are displayed as flutter altitudes in Fig. 6. These altitudes correspond to the ATW operating at a Mach number and its associated flutter speed for a standard atmosphere. The test points are not displayed in Fig. 6, but they are easily noted as conditions of 10,000, 15,000, and 20,000 ft at each Mach number.

The information in Fig. 6 is somewhat easier to disseminate than the corresponding information in Table 2. In particular, it is straightforward to note the accuracy of the different prediction approaches.

Figure 6 clearly demonstrates the adverse sensitivity to poor data quality for the data-based approaches. The damping approach

Table 2 Predicted flutter speeds in feet per second at each Mach number

Mach	V_{damp}	V_{fm}	V_{env}	V_{mu}	V_{arma}	V_{true}
0.55	664	—	732	652	591	660
0.60	657	—	696	697	715	705
0.65	—	—	—	741	2867	749
0.70	780	—	—	782	751	791
0.75	—	843	837	821	806	832
0.80	882	870	884	852	886	871

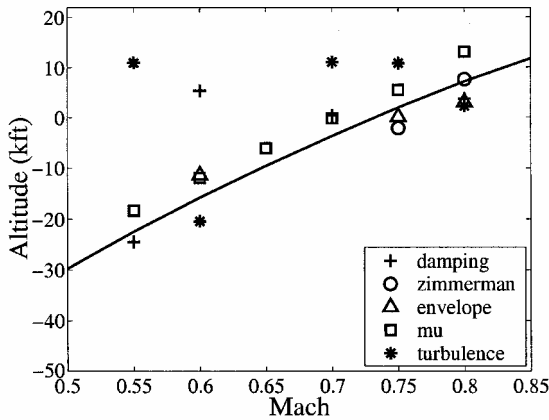


Fig. 6 Predicted flutter speeds during constant-Mach envelope expansion.

computed reasonable predictions at Mach 0.55, 0.70, and 0.80 conditions. The methods based on the flutter margin and the envelope function were able to produce reasonable predictions only at Mach 0.75 and 0.80, which are near the onset of flutter for the flight test. The approach based on ARMA modeling predicted reasonable speeds at Mach 0.60 and 0.80.

Figure 6 also indicates the reduced sensitivity to data quality for the μ -method approach. Essentially, the conservativeness of the predictions remains relatively constant throughout the envelope expansion. The reason for this constancy is that the μ -method approach does not use a curve fit based on observed properties like damping; therefore, this method does not require three high-quality data values. The flutterometer approach is able to observe modeling errors from a single good data set and use this information to update the predicted flutter speed. Test points at which bending is not observed obviously do not relate any information about that mode, and so the μ -method approach simply uses the default level of uncertainty as described by any preceding data sets at that Mach number.

Varying-Mach Predictions

Implementation

Flight data were also analyzed with respect to a varying-Mach envelope expansion. Alternatively, this flight test can be considered as a type of constant-altitude envelope expansion. The objective is to use flight data from all test points, regardless of Mach number, to predict the speed at which flutter will occur for the ATW at an altitude of 10,000 ft.

The approaches used to predict flutter speeds were formulated to be valid for constant-Mach testing; therefore, the algorithms had to be modified for this varying-Mach testing. Essentially, the methods attempted to account roughly for compressibility by considering flutter speed in terms of equivalent airspeed. Specifically, the predictions were given as KEAS.

The data-based prediction methods were straightforward to modify. These methods consider extrapolating functions of flight condition so that the functions were simply altered to reflect characteristics of equivalent airspeed. The functions for the damping method and the envelope method were directly computed as dependent on equivalent airspeed, and so the roots of this function related the flutter speed in KEAS. The functions for the flutter margin method and the ARMA method were still computed as dependent on dynamic pressure; however, the flutter speeds were determined as the equivalent airspeed for the associated roots of those functions using a standard atmosphere.

The model-based prediction method using the μ -method approach and the flutterometer was also modified to reflect the objectives associated with varying-Mach envelope expansion. The modifications consisted of considering a set of models to determine the lowest Mach number at which a model is not robustly stable near 10,000 ft. The assumption behind this approach is that the uncertainty description identified from data at a certain Mach number is a reasonable approximation to the uncertainty at all Mach num-

bers. For instance, as the envelope expansion considers a test point at Mach 0.65, the model at Mach 0.8 is analyzed with respect to uncertainty developed using Mach 0.65 data.

These modifications obviously introduce some error into the predictions. The data-based approaches are clearly not guaranteed to be accurate with respect to airspeed as determined in KEAS. Alternatively, the model-based approach is questionable because of the assumption that the uncertainty levels from one Mach condition are reasonable at any Mach condition. Despite these drawbacks, the predictions are still anticipated to be useful. The main reason for this expectation is that the envelope expansion will only consider subsonic flight. Transonic effects may be noticeable around Mach 0.8, but equivalent airspeed should be an acceptable measure of flight condition for the majority of test points. Obviously, this claim would be highly suspect for larger flight envelopes that include transonic and supersonic flight, and so the current results are considered valid only for this limited flight envelope.

Predictions of Flutter Speed

Predictions of the speed associated with flutter were computed at every test point. These predictions were based on data from the current and any preceding test points. The flutter speeds predicted from each test point are given in Fig. 7 using velocity expressed in KEAS.

The predictions in Fig. 7 demonstrate a general trend that shows the methods are able to predict reasonably accurate flutter speeds; however, it is best for evaluation purposes to consider sets of predictions. Specifically, consider two sets that result from separating the predictions made at test points from less than 350 KEAS and test points with greater than 350 KEAS. Furthermore, consider the model-based flutterometer method separately from the data-based methods based on damping extrapolation, envelope function, Zimmerman–Weissenburger margin,³ and ARMA modeling.

The predictions made using data from low-speed test points of less than 350 KEAS show an interesting behavior. The data-based methods show very poor results at these low-speed test points. The predictions are very scattered in magnitude and do not show any clear trend that could be safely trusted. Furthermore, there are several conditions at which these methods did not predict a valid speed, as evidenced by the lack of markers in Fig. 7.

The predictions made using data that included high-speed test points show a behavior that is very different from the predictions at low-speed test points. Namely, the data-based methods all predict speeds that consistently converge to the correct answer of 460 KEAS. The methods based on damping extrapolation and Zimmerman–Weissenburger³ margins make particularly good predictions. The methods based on envelope function and ARMA modeling show more variations in the predictions, but they clearly converge near the correct answer.

Conversely, the predictions from the flutterometer do not show the same variation with test point airspeed. There is a small decrease in

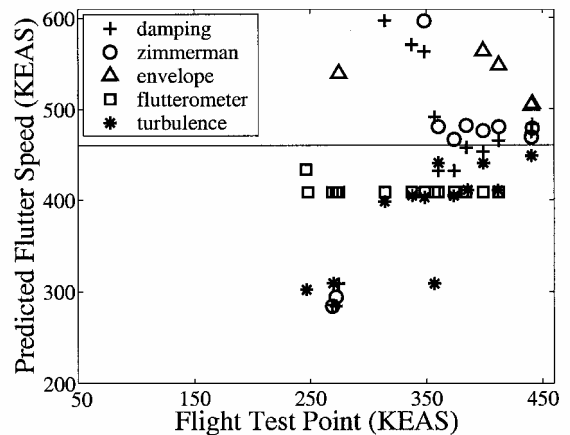


Fig. 7 Predicted flutter speeds during varying-Mach envelope expansion.

predicted speed after the first test point because the tool needs these initial data to update its uncertainty model. The predicted speed shows no variation using data from any other test point.

The predictions in Fig. 7 can be summarized. The data-based methods produce poor predictions using low-speed data, but produce reasonable predictions that converge on the correct answer as the envelope is expanded to include high-speed test points. The flutterometer produces a reasonable worst-case prediction of flutter speed immediately and remains conservative throughout the envelope expansion.

These results are explained by considering the data that were analyzed by each method. The data-based methods, directly or indirectly, use characteristics of the data associated with the modal dampings shown in Fig. 3. These dampings do not indicate any trend toward instability until the test point nears 350 KEAS. Thus, any polynomial based on these data will not predict flutter until the function accounts for data at test points greater than 350 KEAS. The flutterometer does not rely heavily on these damping values; rather, it combines both data and theoretical models. The flutterometer was able to identify an uncertainty description for the model by analyzing data at the first test point. The data from other test points did not indicate any more errors, and so the flutter margin does not show dependence on test point.

The analysis of Fig. 7 agrees with the nature of the prediction methods. Namely, the data-based methods attempt to compute the exact speed associated with the onset of flutter, whereas the flutterometer attempts to compute a conservative prediction of the worst-case flutter speed. It is expected that the data-based methods should be highly accurate at test points that are close to flutter. It is also expected that this implementation of the flutterometer should not reduce conservatism despite analyzing data from high-speed test points.

Also, the analysis indicates the sensitivity of the methods. The data-based methods are formulated using optimality criterion, and so they are highly susceptible to errors in the data. Conversely, the flutterometer is formulated using a robust criterion, and so it is much less sensitive to variations in data.

Conclusions

This paper has evaluated several methods to predict the onset of flutter. In particular, data-based approaches that only analyze flight data are compared with a model-based approach that analyzes flight data in conjunction with a theoretical model. Flight data from the ATW have been used for this evaluation. At low speeds, the data-based approaches were unable to predict the onset of flutter consistently with any accuracy, whereas the model-based flutterometer was able to predict a reasonable estimate of the flutter speed. At high speeds, the data-based approaches converged to an accurate prediction, whereas the model-based flutterometer predicted a flutter speed that was conservative. One reason for these results is that the flight data were of limited quality at low-speed test points and the data-based approaches were particularly susceptible to this problem. Another reason for these results is that this implementation of

the flutterometer did not update the baseline model, and so it was unable to take advantage of information from high-speed test points and converge to the true flutter speed.

The predicted speeds suggest a method for envelope expansion can be formulated that uses the various methods. The flight test should be initiated using the flutterometer at the low-speed test points to get an initial conservative estimate of the flutter speed. The flight test would proceed using the flutterometer estimates until the test points approach the predicted speed. The envelope expansion at high-speed should rely more heavily on the data-driven methods to finalize an accurate prediction of the exact speed at which flutter will be encountered. Of course, the envelope expansion must still proceed with extreme caution, but the combination of these approaches will possibly allow for a more efficient flight-test program.

References

- ¹Kehoe, M. W., *A Historical Overview of Flight Flutter Testing*, NASA TM-4720, Oct. 1995.
- ²Cooper, J. E., Emmett, P. R., Wright, J. R., and Schofield, M. J., "Envelope Function: A Tool for Analyzing Flutter Data," *Journal of Aircraft*, Vol. 30, No. 5, 1993, pp. 785-790.
- ³Zimmerman, N. H., and Weissenburger, J. T., "Prediction of Flutter Onset Speed Based on Flight Testing at Subcritical Speeds," *Journal of Aircraft*, Vol. 1, No. 4, 1964, pp. 190-202.
- ⁴Lind, R., and Brenner, M., "Flutterometer: An On-Line Tool to Predict Robust Flutter Margins," *Journal of Aircraft*, Vol. 37, No. 6, 2000, pp. 1105-1112.
- ⁵Torii, H., and Matsuzaki, Y., "Flutter Margin Evaluation for Discrete-Time Systems," *Journal of Aircraft*, Vol. 38, No. 1, 2001, pp. 42-47.
- ⁶Dimitriadis, G., and Cooper, J. E., "Flutter Prediction from Flight Flutter Test Data," *Journal of Aircraft*, Vol. 38, No. 2, 2001, pp. 355-367.
- ⁷Shelley, S. J., and Pickrel, C. R., "New Concepts for Flight Flutter Parameter Estimation," *International Modal Analysis Conference*, Society for Experimental Mechanics, Bethel, CT, Feb. 1997, pp. 490-496.
- ⁸Pitt, D. M., "Flutter Margin Determination for Single Degree-of-Freedom Aeroelastic Instabilities," *International Forum on Aeroelasticity and Structural Dynamics*, Asociacion de Ingenieros Aeronauticos de Espana, Madrid, Spain, June 2001, pp. 321-332.
- ⁹Price, S. J., and Lee, B. H. K., "Evaluation and Extension of the Flutter-Margin Method for Flight Flutter Prediction," *Journal of Aircraft*, Vol. 30, No. 3, 1993, pp. 395-402.
- ¹⁰Bennett, R. M., *Application of Zimmerman Flutter-Margin Criterion to a Wind-Tunnel Model*, NASA TM-84545, Nov. 1982.
- ¹¹Lind, R., and Brenner, M., *Robust Aeroservoelastic Stability Analysis*, Springer-Verlag, London, April 1999, pp. 55-116.
- ¹²Matsuzaki, Y., and Ando, Y., "Estimation of Flutter Boundary from Random Responses due to Turbulence at Subcritical Speeds," *Journal of Aircraft*, Vol. 18, No. 10, 1981, pp. 862-868.
- ¹³Torii, H., and Matsuzaki, Y., "Flutter Boundary Prediction Based on Nonstationary Data Measurement," *Journal of Aircraft*, Vol. 34, No. 10, 1997, pp. 427-432.
- ¹⁴Balas, G. J., Doyle, J. C., Glover, K., Packard, A., and Smith, R., *μ -Analysis and Synthesis Toolbox—Users Guide*, The MathWorks, Natick, MA, 1991, pp. 2:27-2:33.
- ¹⁵Lind, R., "Flight Testing with the Flutterometer," AIAA Paper 01-1654, April 2001.
- ¹⁶Ljung, L., *System Identification Toolbox—Users Guide*, The MathWorks, Natick, MA, 1995, pp. 3:25-3:28.